2D TOMOGRAPHY FOR VSP

J. L. Guiziou, Y. Dezard and G. Martayan

ABSTRACT

Tomography for VSP recovers a layered image of the earth from the traveltimes of borehole seismic surveys. Coupling an analytical two-point ray-tracing algorithm with continuation methods leads to fast and accurate computation of traveltimes. The parametrization of the model by B-splines enables the use of a fast and stable inversion process, using a nonlinear inverse theory. Test cases demonstrate the reliability of the method.

INTRODUCTION

Migration has now become a major seismic-data processing tool leading to an accurate earth image on which interpretation is based. However, the result of migration remains highly dependent on the input velocity model and the velocity estimation is the toughest part of the job. Many people are working on velocity- analysis methods now and tomography is one of those methods.

This paper presents the approach that we followed at TOTAL CFP to deal with VSP tomography in the general case of a two dimensional layered medium. The aim of that work was to propose a tool allowing the interpreter to extend his knowledge as far as possible in the surroundings of a borehole.

We will see which geological medium can be considered and how that medium is parametrized. Because we wanted to obtain significant interactivity on a mini-computer (e.g. HP9000), we developed an efficient ray-tracing routine, based on continuation, and we chose an inversion algorithm leading to fast convergence. A few examples illustrate the reliability of the method, which is worth being extended to surface seismic data.

Our approach to the geological medium

A commonly used representation of the geological medium is that of velocity cells (Bishop et al., 1985), but we preferred to represent our model by a superposition of layers of various shapes and thicknesses. The velocity discontinuity between two adjacent layers is represented by a continuous curve of arbitrary shape (see Figure 1). This approach enables to figure out important velocity discontinuities resulting from faults, domes or pinch-outs. We allow the velocity to vary within each layer; this capability is interesting when we consider the problem of sub-surface lateral anomalies, for instance.

Now, how to parametrize that geological model ? Tomography is typically an inversion of a set of traveltimes, so we must be aware that the model's parametrization will highly influence the inversion results in terms of stability, computational cost, speed of convergence, etc. We choose to parametrize each depth horizon (interface between two layers) and each velocity profile (within a layer) by a B-splines curve (see Figure 1).

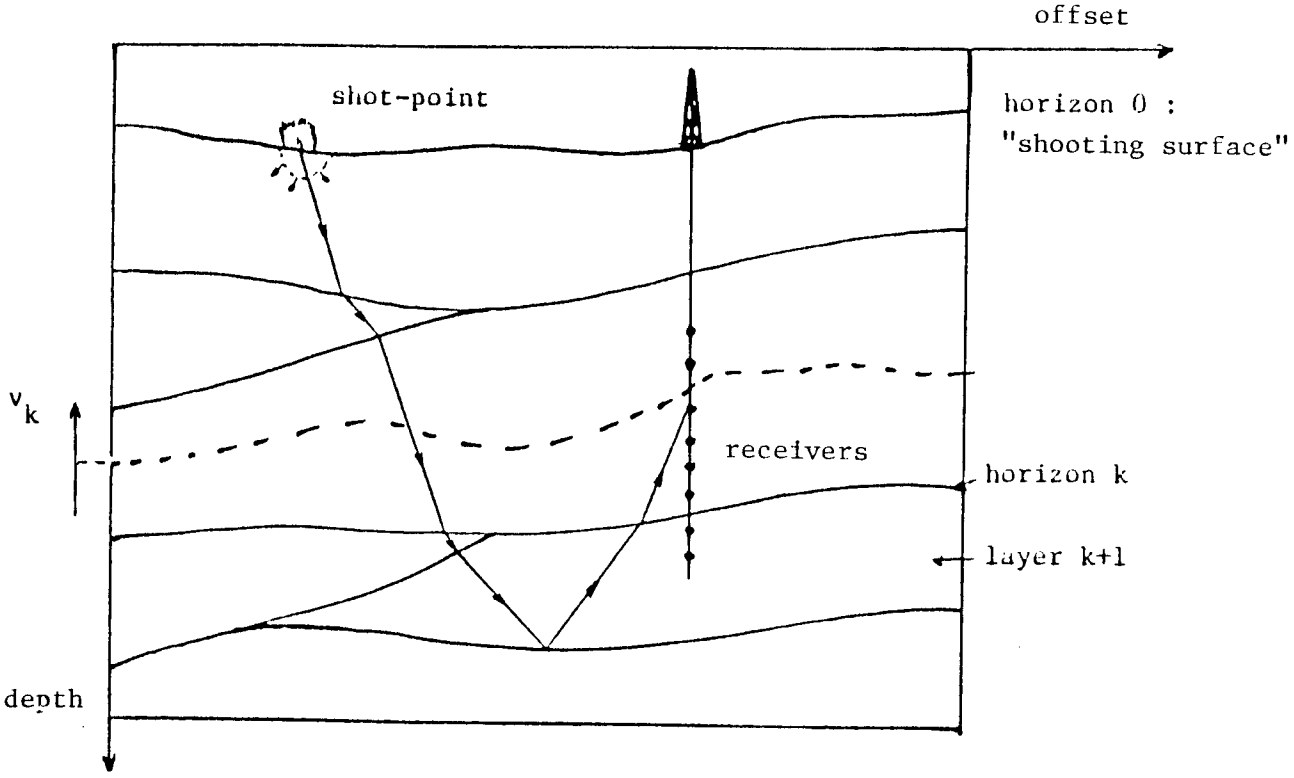

FIG. 1. Layered model of the geological medium.

Figure 2 illustrates the construction of a B-splines interpolator C(x). Given the set of digitized points representing the horizon in the offset-depth domain (x,z), the algorithm defines a finite set of knots $N = (n_1,...,n_i,...,n_M)$ regularly or irregularly spaced along the x-axis and a finite set of coefficients $A = (\alpha_1, \ldots, \alpha_i, \ldots, \alpha_M)$ associated to the knots (Diercks, P.). Then the computation of the z-axis value $C(x_0)$ for a given abscissa x_0 is merely a linear combination of a few parameters α_i weighted by local basis functions $B_{.,k}(x)$.
This gives the following relation :

$$C(x_0) = \sum_{j=i-k}^{i} \alpha_j B_{j,k}(x_0) \quad , \quad x_0 \in (x_i, x_{i+1}) \quad , \tag{1}$$

where k is the degree of the spline and

$B_{j,k}(x_0)$ is the value, at x_0, of the basis function $B_{j,k}(x)$ associated with parameter α_j.

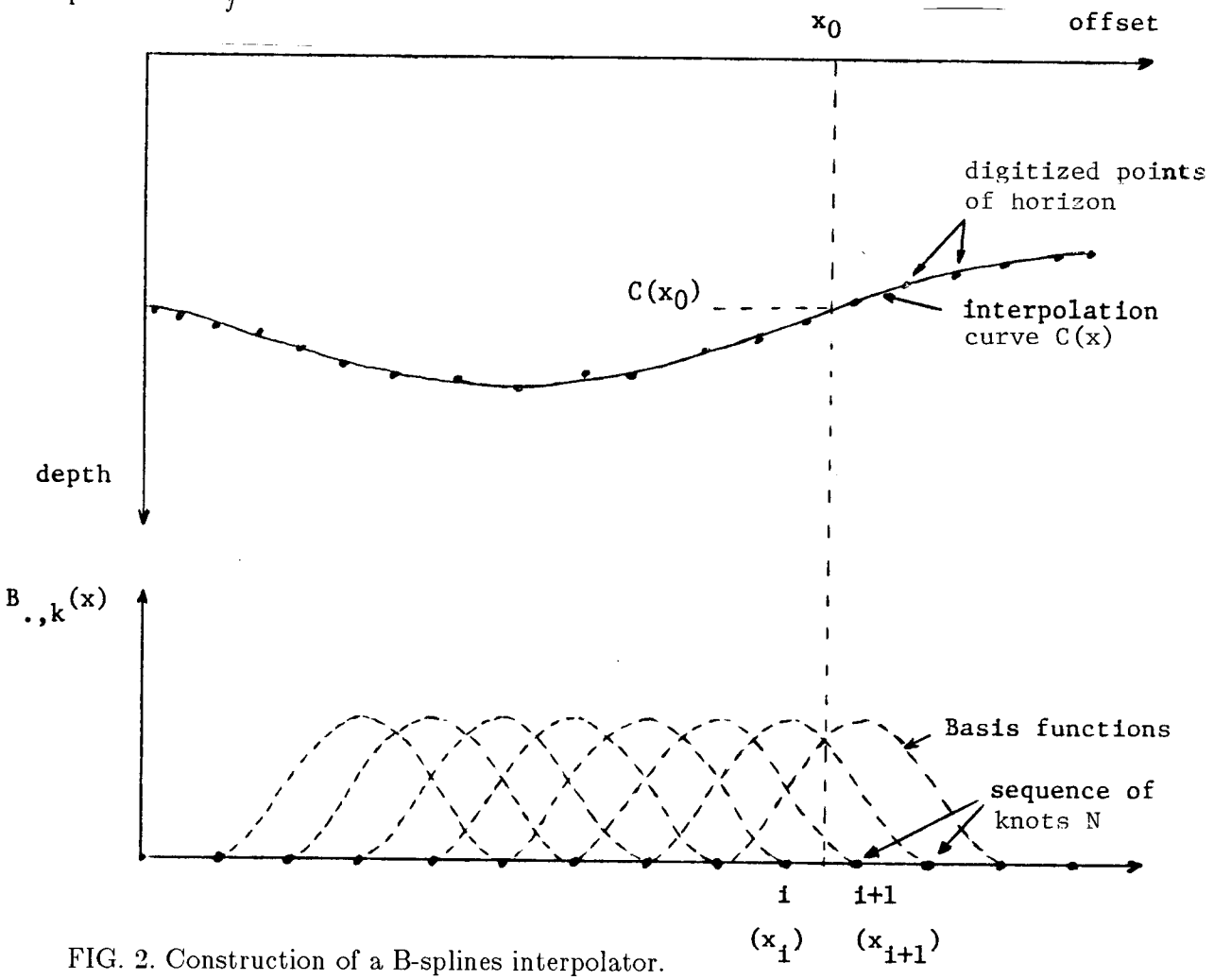

FIG. 2. Construction of a B-splines interpolator.

The B-splines present several advantages for our purpose of tomography :

- First, they are **local** interpolators: only a few knots are involved in the computation of $C(x_0)$. This characteristic is helpful for the efficiency of the Jacobian matrix computation.

- Since they are **non-exact** interpolators, they are not inclined to produce unexpected oscillations, which are severely critical in ray-tracing.

- Such a parametrization leads to a limited number of parameters and consequently **limits the unknowns** of our inverse problem.

Three types of seismic surveys

The tomographic procedure can be applied to three major types of borehole surveys, namely the Vertical Seismic Profile (VSP), the Offset or Multi-offsets VSP and the Walk-Away. The VSP and Offset-VSP acquisitions involve a limited number of shot-points located on the surface of the earth and a large number of receivers (60 to 100) set in the borehole. As we can see on Figure 3, this survey geometry mainly investigates deep events, often situated below the maximum depth of the well.

The Walk-Away survey (Figure 4) enables a better lateral investigation than does the VSP. In this case, the wave fronts are recorded on few receivers (5 to 7) but there are many shot-point locations displayed on both sides of the well. These traveltimes data can help to solve problems due to sub-surface anomalies.

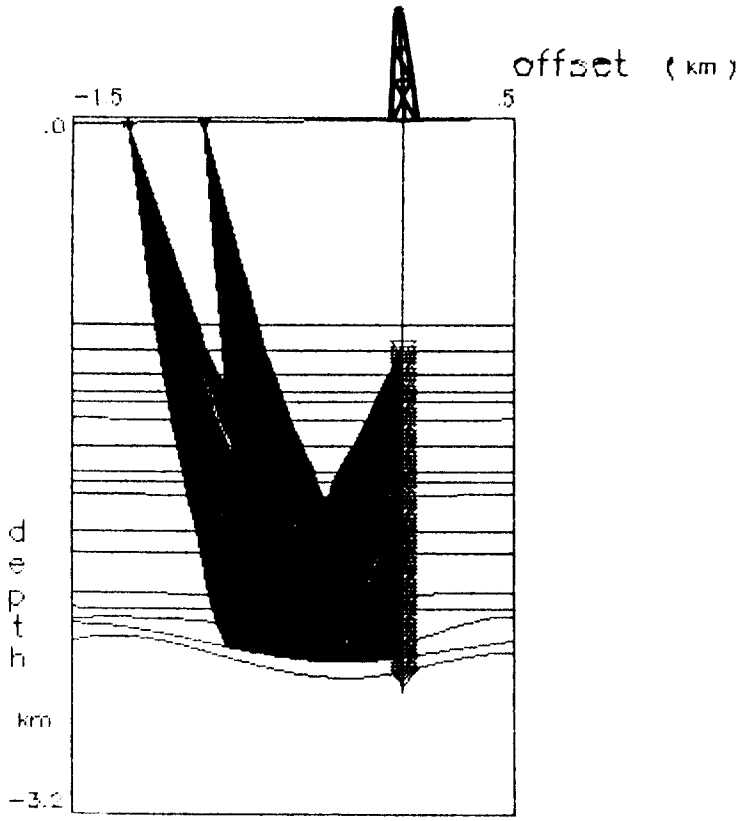

FIG. 3. Two offsets Vertical Seismic Profile.

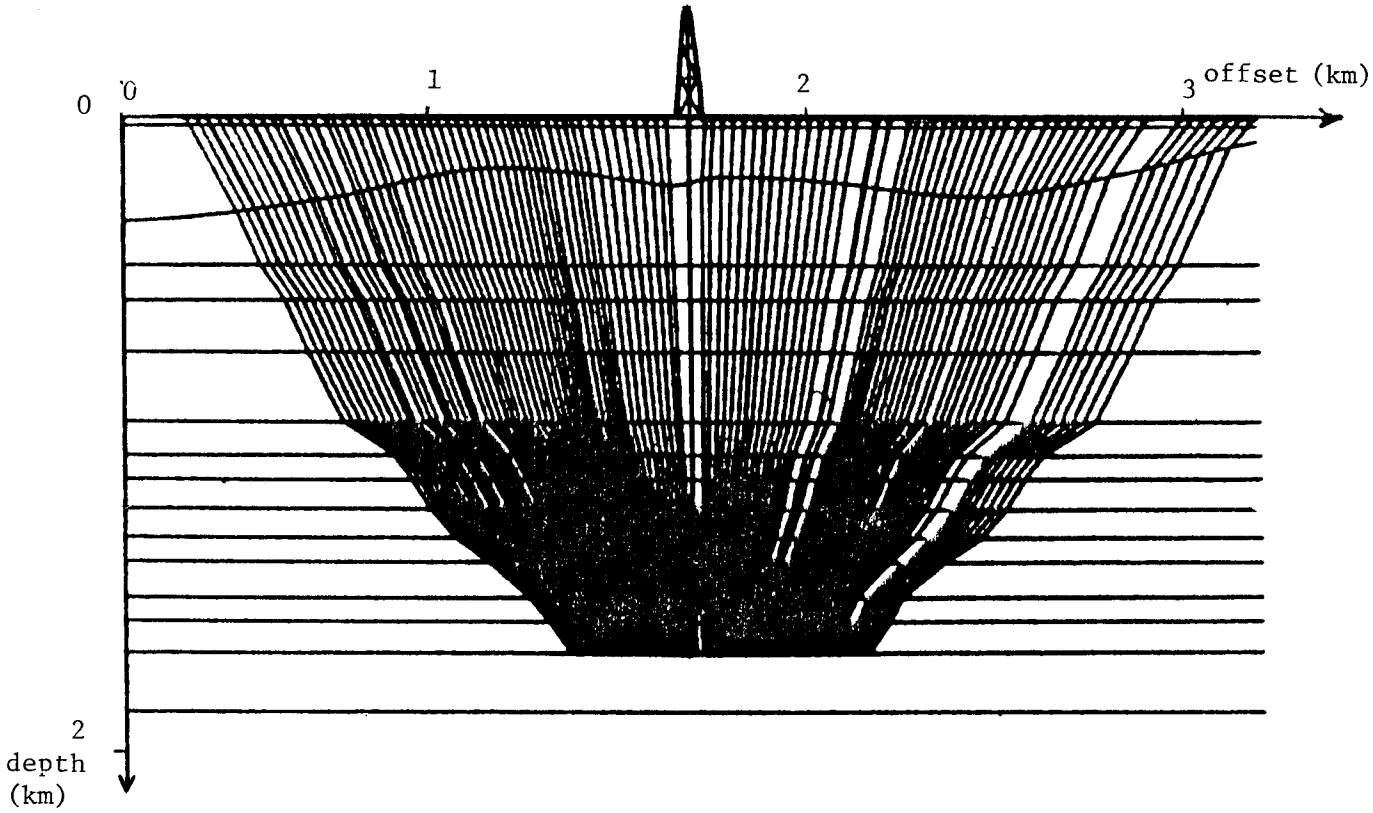

FIG. 4. Walk-Away survey.

Ray-tracing routine

In order to obtain an interactive tomographic procedure, we have to develop a computationally efficient ray-tracing algorithm. The algorithm is also supposed to compute accurate traveltimes and to allow a fast and precise computation of the Jacobian matrix.

We base our ray-tracing algorithm on the work of H.B. Keller and D.J. Perozzi (Keller and Perozzi, 1983) who introduced a new method of ray computation in seismology. Given a set of shot points, receivers, and reflectors, rays are computed sequentially in an efficient way by solving non-linear systems with the help of continuation procedures.

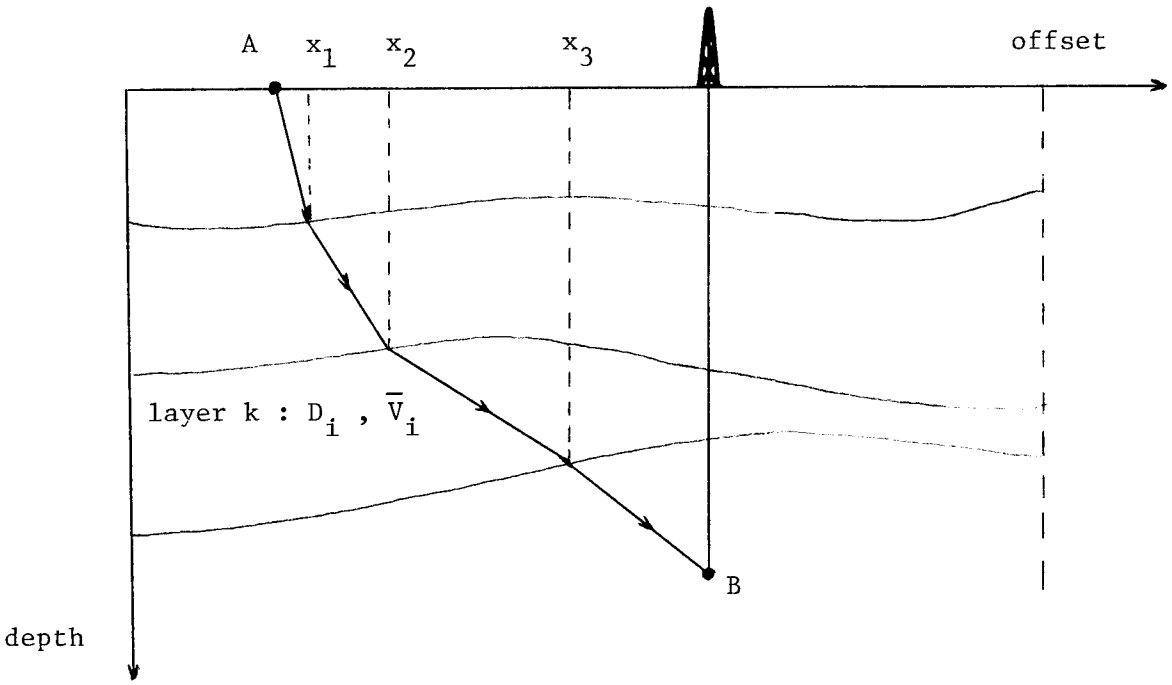

FIG. 5. Ray-tracing formulation

Suppose we want to determine the raypath between two points A and B, as displayed on Figure 5. For a given depth model, we are supposed to be able to determine how many horizons will be intersected by the ray and which these horizons are. If we assume that this has been solved, our raypath will be completely determined by the vector $X = (x_0, \ldots, x_i, \ldots, x_{n+1})^T$ of x-axis positions of intersection points between the ray and the horizons, leading to a broken line that satisfies the *Fermat* principle.

An important point is that although our geological model has possible variable velocities $v_k(x)$, we assume that along the raypath, within a given layer k, the ray travels at a constant seismic velocity $\overline{V}_i$, which can be computed as a mean velocity between velocities at the enter and exit points of the ray in the layer.

Let t be the traveltime of a ray crossing n+1 layers :

$$t = \sum_{i=1}^{n+1} t_i(x_{i-1}, x_i) \quad , \tag{2}$$

$$with \begin{cases} x_0 = shot\ point \\ x_{n+1} = receiver \end{cases} .$$

The elementary traveltime $t_i(x_{i-1}, x_i)$ across a layer k is defined as follows :

$$t_i(x_{i-1}, x_i) = \frac{D_i(x_{i-1}, x_i)}{\overline{V}_i(x_{i-1}, x_i)} \quad , \tag{3}$$

with $D_i(x_{i-1}, x_i) =$ travel distance within layer k.

The appropriate vector X is defined by the Fermat principle :

$$\frac{\partial t}{\partial X} = 0 .$$

This leads to a vectorial function : $\Phi = \begin{bmatrix} \phi_1 \\ \phi_2 \\ \vdots \\ \phi_n \end{bmatrix}$ each component of which, ϕ_i, can be written as :

$$\phi_i(x_{i-1}, x_i, x_{i+1}) = \frac{\partial t_i(x_{i-1}, x_i)}{\partial x_i} + \frac{\partial t_{i+1}(x_{i+1}, x_i)}{\partial x_i} = 0 \quad , \ i = 1, n \ .$$

The solution vector X is obtained by solving the non-linear system :

$$\Phi(X) = 0 .$$

Therefore, we use the Newton iterative procedure. Given an approximation $X^\nu = ({x_1}^\nu, \ldots, {x_n}^\nu)^T$ of X at step ν, a more accurate approximation $X^{\nu+1} = X^\nu + \Delta X^\nu$ can be obtained as follows :

$$\Phi(X^{\nu+1}) = \Phi(X^\nu) + \Delta X^\nu \frac{\partial \Phi(X^\nu)}{\partial X^\nu} = 0 , \tag{4}$$

An important point is that although our geological model has possible variable velocities $v_k(x)$, we assume that along the raypath, within a given layer k, the ray travels at a constant seismic velocity $\overline{V}_i$, which can be computed as a mean velocity between velocities at the enter and exit points of the ray in the layer.

Let t be the traveltime of a ray crossing n+1 layers :

$$t = \sum_{i=1}^{n+1} t_i(x_{i-1}, x_i) \quad , \tag{2}$$

$$with \begin{cases} x_0 = shot\ point \\ x_{n+1} = receiver \end{cases} .$$

The elementary traveltime $t_i(x_{i-1}, x_i)$ across a layer k is defined as follows :

$$t_i(x_{i-1}, x_i) = \frac{D_i(x_{i-1}, x_i)}{\overline{V}_i(x_{i-1}, x_i)} \quad , \tag{3}$$

with $D_i(x_{i-1}, x_i) =$ travel distance within layer k.

The appropriate vector X is defined by the Fermat principle :

$$\frac{\partial t}{\partial X} = 0 .$$

This leads to a vectorial function : $\Phi = \begin{bmatrix} \phi_1 \\ \phi_2 \\ \vdots \\ \phi_n \end{bmatrix}$ each component of which, ϕ_i, can be written as :

$$\phi_i(x_{i-1}, x_i, x_{i+1}) = \frac{\partial t_i(x_{i-1}, x_i)}{\partial x_i} + \frac{\partial t_{i+1}(x_{i+1}, x_i)}{\partial x_i} = 0 \quad , \ i = 1, n \ .$$

The solution vector X is obtained by solving the non-linear system :

$$\Phi(X) = 0 .$$

Therefore, we use the Newton iterative procedure. Given an approximation $X^\nu = ({x_1}^\nu, \ldots, {x_n}^\nu)^T$ of X at step ν, a more accurate approximation $X^{\nu+1} = X^\nu + \Delta X^\nu$ can be obtained as follows :

$$\Phi(X^{\nu+1}) = \Phi(X^\nu) + \Delta X^\nu \frac{\partial \Phi(X^\nu)}{\partial X^\nu} = 0 , \tag{4}$$

$$\frac{\partial \Phi(X^{\nu})}{\partial X^{\nu}} \quad \text{being a tri-diagonal matrix .}$$

We can see that this Newton procedure requires an initial guess X^0 of the solution. Here is the point at which continuation is useful: it allows us, using a neighbor ray, to deduce easily an X^0 close to the solution. The continuation consists of an extrapolation of a solution vector X from a given state of parameters (old ray) to another state of parameters (new ray) (Figure 6).
The efficiency of the ray-tracing algorithm is determined by the application of the continuation procedure to the right parameters, depending on the acquisition survey to be modelized.

To our VSP seismic data, we applied mainly the continuation on the receivers locations. For instance, the extrapolation of the solution vector X from a receiver R_1 to the next receiver R_2 can be written as

$$R(\lambda) = \lambda * R_2 + (1-\lambda) * R_1 \quad , \lambda \in [0,1] .$$

We can infer a solution guess $X^0(\lambda+\Delta\lambda)$, at step $\lambda+\Delta\lambda$, from the solution $X^0(\lambda)$, at step λ, as follows :

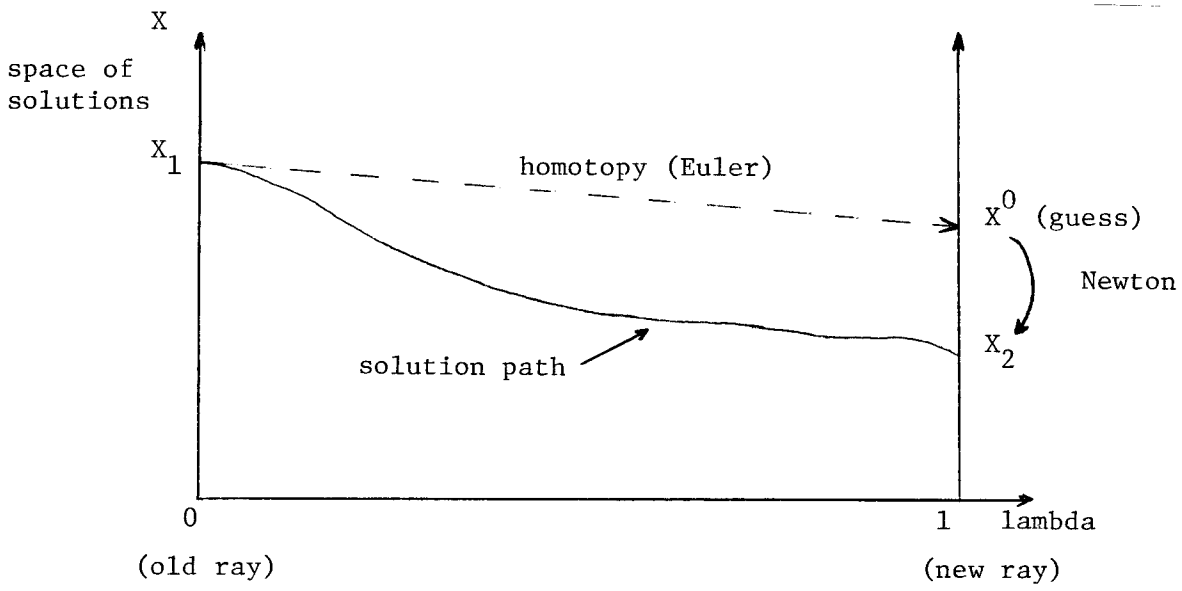

FIG. 6. Illustration of the continuation technique.

$$X^0(\lambda+\Delta\lambda) = X^0(\lambda) + \Delta\lambda \dot{X}^0(\lambda) \ ; \ \dot{X}^0(\lambda) = \frac{\partial X^0(\lambda)}{\partial \lambda} \ .$$

The vector $X^0(\lambda)$ is supposed to satisfy the equation

$$\Phi \ (X^0(\lambda),\lambda) = 0 \ ,$$

so that we can write

$$\frac{\partial \Phi}{\partial \lambda} = \frac{\partial \Phi}{\partial X^0}\frac{\partial X^0}{\partial \lambda} + \frac{\partial \Phi}{\partial \lambda} = 0 \ ,$$

$$hence \ \ \dot{X}^0(\lambda) = - \frac{\partial \Phi}{\partial X^0}\frac{\partial \Phi}{\partial \lambda}$$

We recognize $\frac{\partial \Phi}{\partial X^0}$ as the tri-diagonal matrix of equation (4).

If the continuation is applied on the receivers, the entity $\frac{\partial \Phi}{\partial \lambda} = (\frac{\partial \phi_1}{\partial \lambda}, \ . \ . \ . \ , \frac{\partial \phi_n}{\partial \lambda})$ simplifies to :

$$\frac{\partial \phi_n}{\partial \lambda} = (x_{r\,2}-x_{r\,1})\frac{\partial \phi_n}{\partial x_r} + (z_{r\,2}-z_{r\,1})\frac{\partial \phi_n}{\partial z_r} \ , \qquad (5)$$

$$with \quad \begin{cases} \dfrac{\partial \phi_n}{\partial x_r} = \dfrac{\partial}{\partial x_r}\left[\dfrac{\partial t_{n+1}}{\partial x_n}\right] \\ \dfrac{\partial \phi_n}{\partial z_r} = \dfrac{\partial}{\partial z_r}\left[\dfrac{\partial t_{n+1}}{\partial z_n}\right] \end{cases} .$$

In general, only one continuation step $\Delta\lambda = 1$ is needed to obtain a satisfying approximate solution for the new ray.

Inversion procedure

After the computation of the traveltimes on a given geological model, we propose to perturb the model parameters (i.e. the B-splines coefficients) so that our set of traveltimes best fits the set of survey-observed traveltimes. The inversion algorithm that we use is a slight variation of the one proposed by Tarantola and Valette (1982), so that we can tune the influence of the initial model on the inversion result. The algorithm is based on the following equation :

$$p_{k+1} = p_k + (G_k{}^T . C_{d\,0}{}^{-1} . G_k + C_{p_0}{}^{-1})^{-1} . \left\{ G_k{}^T . C_{p_0}{}^{-1} . \left[d_0 - g\,(p_k) \right] - C_{p_0}{}^{-1} . \frac{(p_k - p_0)}{\alpha} \right\}$$

p_0 : initial model parameters

p_k : k-th iteration solution

$d_0 - g(p_k)$: difference between observed and computed data
G_k : Jacobian matrix at iteration k
C_{p_0} : covariance matrix on model parameters
C_{d0} : covariance matrix on observed data
α : weight coefficient on initial model

Two pieces of information must be provided to the algorithm :

- the observed traveltimes and their reliability, and
- some a priori information on a "reasonable" geological model.

The Jacobian matrix G_k is computed analytically at the same time as are the traveltimes. The low computational cost enables us to update this matrix at each iteration. This inversion algorithm leads to a fast convergence, because fewer than five iterations generally provide a satisfying result. We can use several criteria to judge the quality of the solution obtained at each iteration. Among those criteria, the standard deviation measuring the difference between the observed and computed traveltimes, and the interpreter's visual analysis of the result are the most commonly used.

Applications to synthetic data

The algorithm was applied to two sets of synthetic data. These examples are only an illustration of what we can expect from this VSP tomographic procedure. They show that the method is reliable; examples on real data that have been carried out at TOTAL CFP also confirm the method's reliability.

Restitution of pinch-outs.— Figure 7 shows the geological model that we try to recover with tomography. We assume that there are 15 shot-points on the surface of the earth and 10 receivers located in the well. Our main objective is a good restitution of the pinched layer situated under the borehole. Velocities within the layers are assumed to be constant. The traveltimes computed on that model will be referred to as "correct data".

We consider the geological starting guess displayed on Figures 8.a and 8.b. We have modified the velocities in layers three and four as well as the horizons three and four, so that the pinch-outs do not appear any more. The traveltimes computed on that geological model lead to an 80 millisecond standard deviation with respect to the correct data.

The result of the first iteration of the inversion is displayed in Figure 9. We can see that the two unknown horizons have moved close to their expected positions, despite the remaining error in the unknown velocities. The second iteration leads to a satisfying result for both horizon shapes and velocity values (Figure 10). The standard deviation on traveltimes has decreased to 1.8 ms, with respect to the correct model. The pinch-outs are fairly well recovered, despite the combined inversion of both horizons and interval velocities.

Restitution of a dome location.— The next example shows that the method can properly reconstruct a correct model from synthetic data derived from that model. In particular, the starting guess will misplace a dome, which will then be properly repositioned by the inversion method. The seismic layout is similar to that of the above example and we still assume that velocities remain constant along the x-axis (see Figure 11.a). Figure 11.b displays the geological area actually reached by the rays and we must keep in mind that tomographic results will be relevant for only this region of the earth.

Our starting guess for the geological model differs from the correct one in the sense that we misplace the dome with respect to the borehole. Besides that, we consider that the velocities are correct. This initial model and the related raypaths are displayed in Figures 12.a and 12.b.

Three inversion iterations are sufficient to improve the traveltimes fitness from a 70 ms standard deviation down to a 0.7 ms one. The dome flank has moved fairly close to its correct position, where layers two and three are pinched out (Figures 13.a and 13.b). Figure 14 displays the aspect of the seismogram, recorded at the first receiver, corresponding to the correct model, the initial guess and the tomography result.

CONCLUSION

The development of this tomographic procedure shows that both modeling and inversion algorithms can be found to provide an interactive tool for velocity analysis. The borehole seismic data studied here is of course a specific one, but it allows us to draw conclusions for an adaptation of the method to the general case of surface data. One of the most promising features is the layered parameterization of the geological model. This model conception, especially when used with local interpolators such as B-splines, simplifies and stabilizes the tomographic inversion. Also, the analytical ray-tracing algorithm allows rather easy modifications in order to improve the geological model, for example by including anisotropy. An expected issue in the generalization to surface data could be that of non-unique two-point traveltimes but we hope that this question can be overcome in a reasonable way.

ACKNOWLEDGEMENTS

Jean Luc Guiziou is indebted to TOTAL CFP for his stay and study at Stanford.

REFERENCES

Bishop, T. et al., 1985, Tomographic determination of velocity and depth in laterally varying media. Geophysics, 50.

Diercks, P., 1975, An algorithm for smoothing, differentiation and integration of experimental data using splines functions. J.Comp.Appl. Maths 1, 165-184.

Diercks, P., 1981, An improved algorithm for curve fitting with spline functions. Report TW 54, July 1981, Department of Computer Science, Katholieke Universiteeit Leuven (Belgium).

Keller, H.B. and Perozzi, D.J., 1983, Fast seismic ray-tracing. SIAM, Vol. 43, n. 4, August, 1983.

Tarantola, A. and Valette, B., 1982, Generalized non-linear inverse problems solved using the least square criterion. Rev. Geophys. Space Phys., 20(2), 219-232.

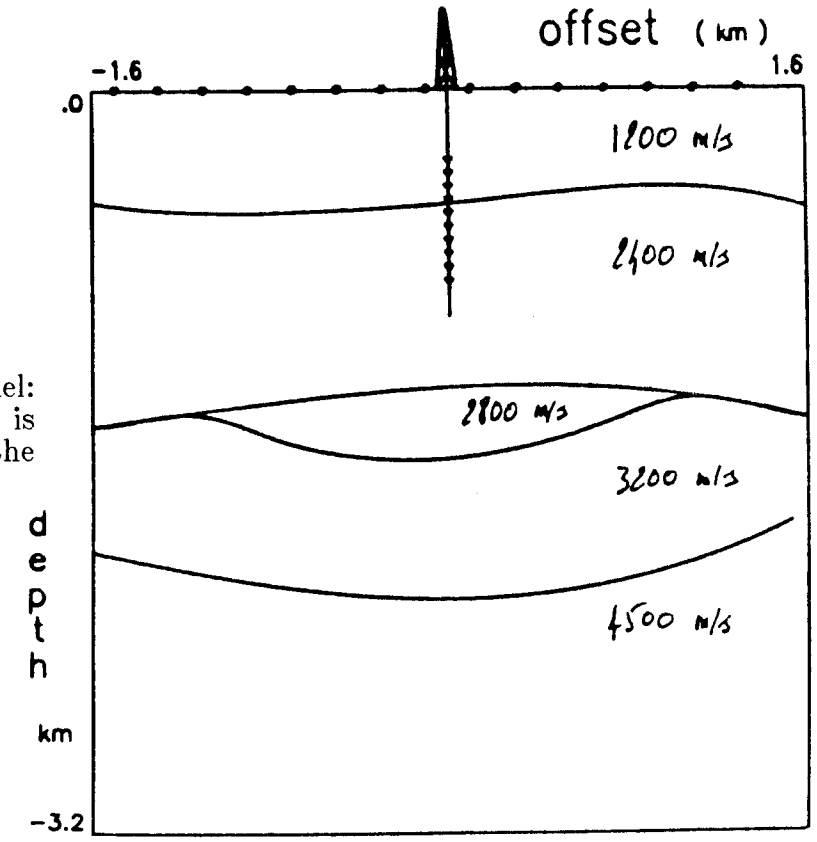

FIG. 7. Synthetic model: the inversion target is situated under the borehole.

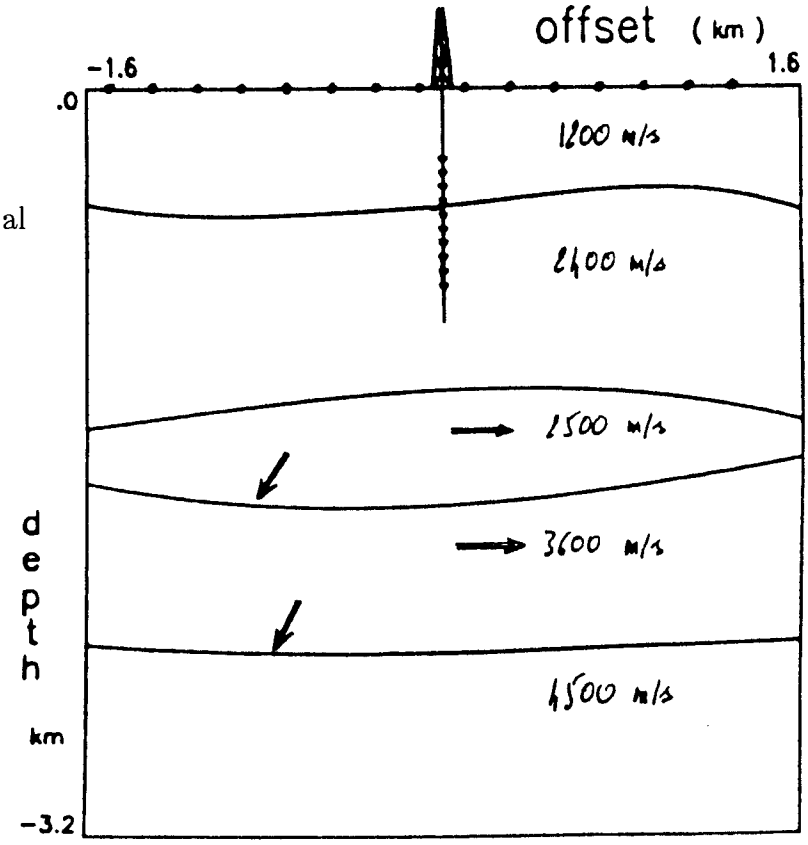

FIG. 8.a. Initial geological model.

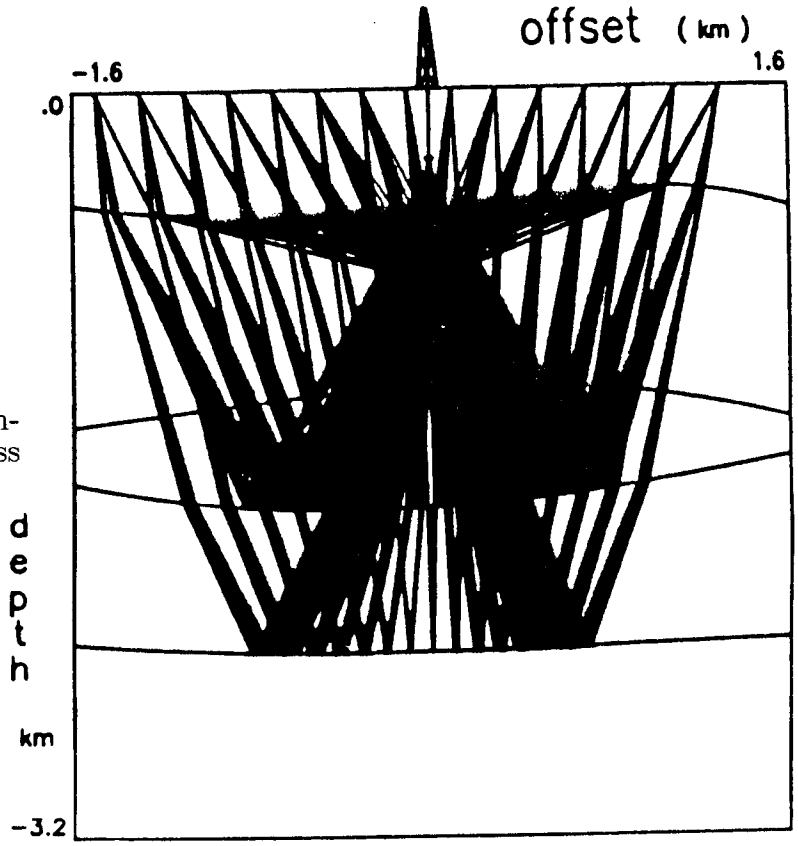

FIG. 8.b. Raypaths computed on the starting guess model.

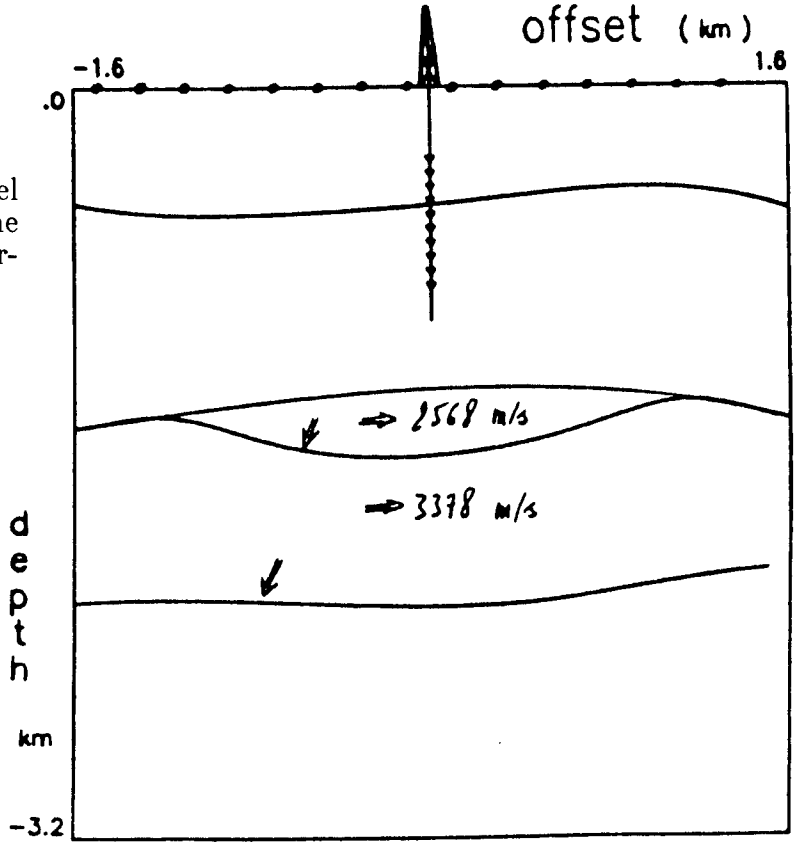

FIG. 9. Geological model after one iteration. The main trend of the interfaces is recovered.

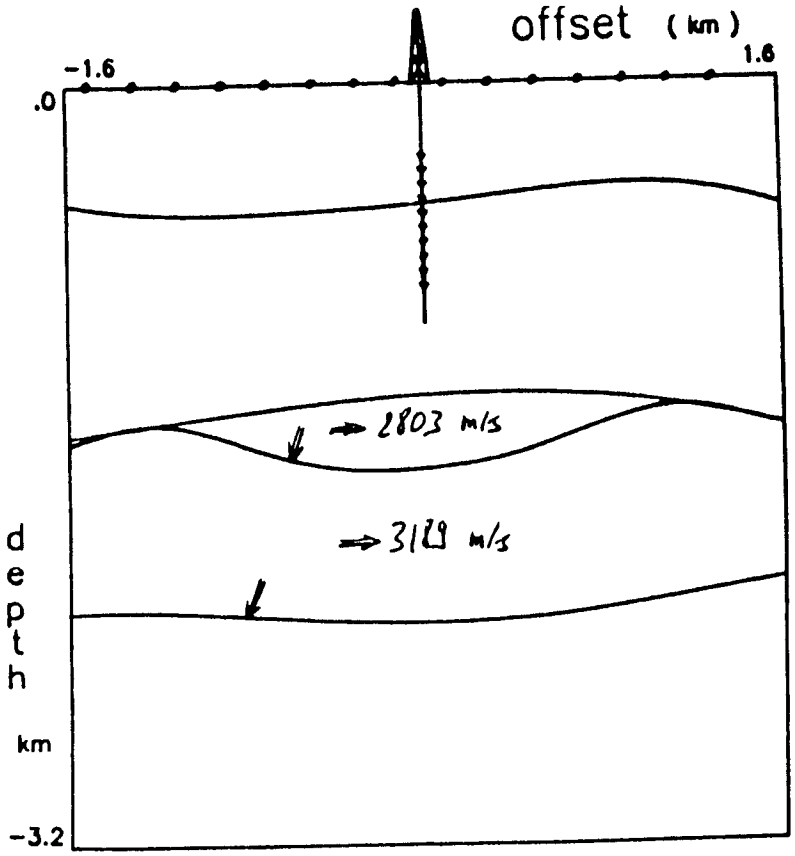

FIG. 10. Two iterations were sufficient to provide a good restitution of the geological model considered.

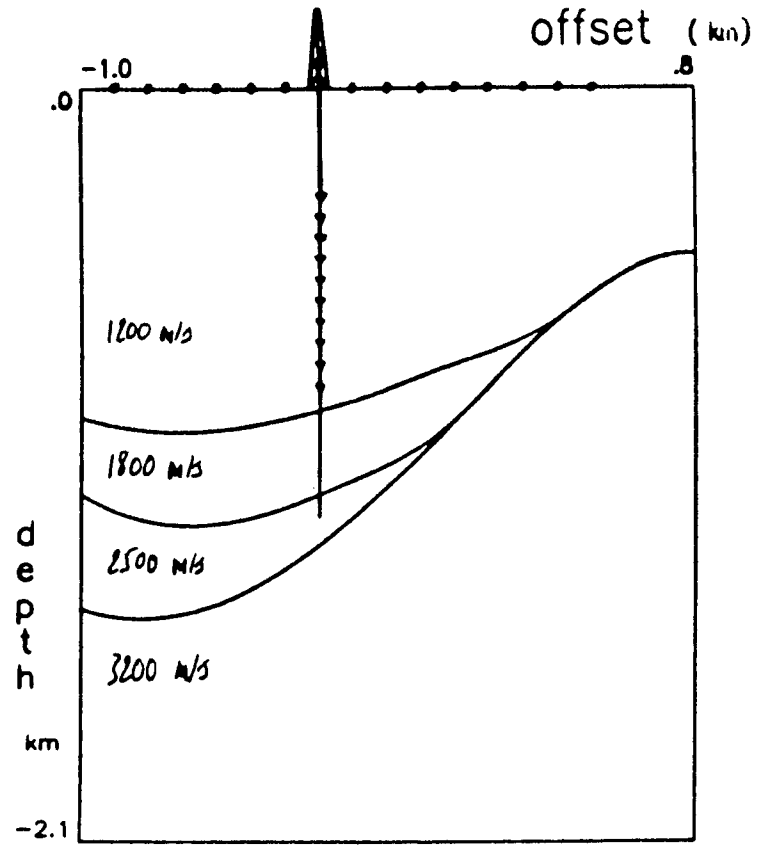

FIG. 11.a. Inversion of a dome location. Correct model.

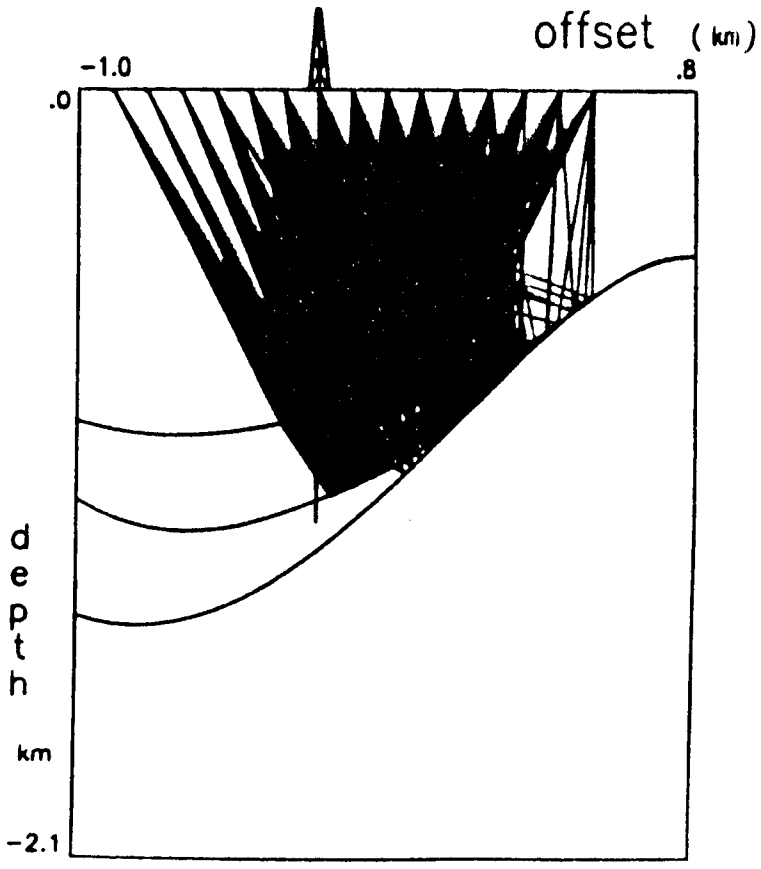

FIG. 11.b. Raypaths computed on the correct model. We can notice the limited area reached by the rays.

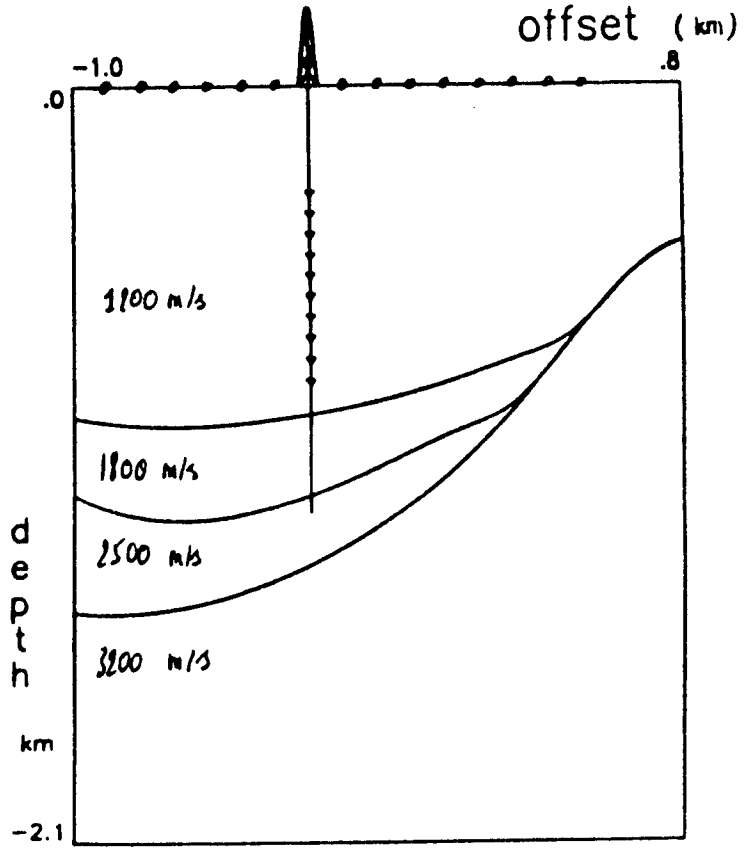

FIG. 12.a. Dome position starting guess. The relative positions of the pinch-outs, with respect to the borehole, are misplaced.

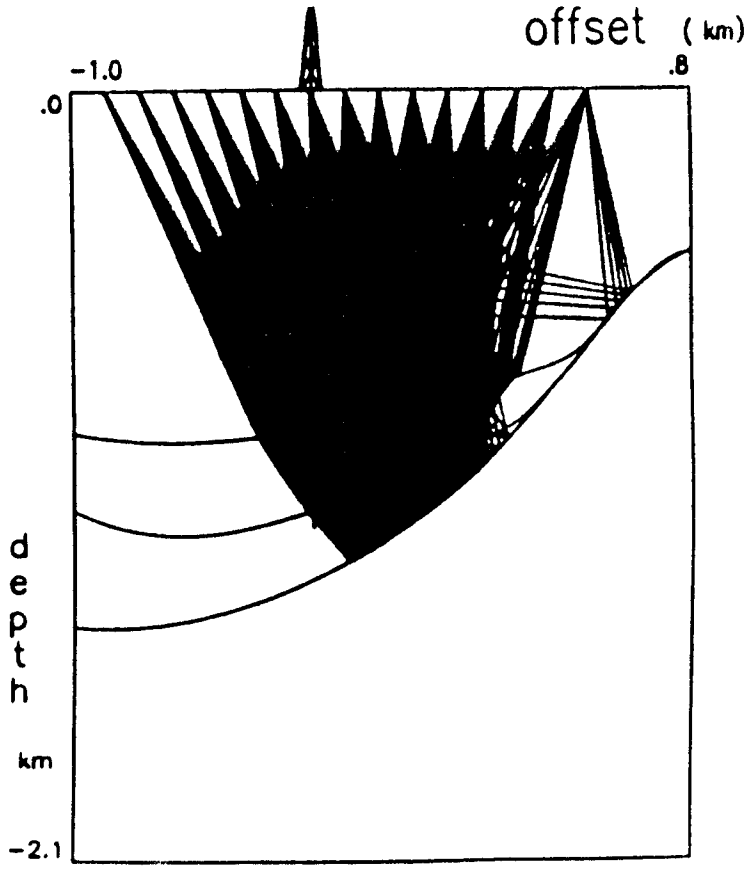

FIG. 12.b. Raypaths computed on the starting guess model.

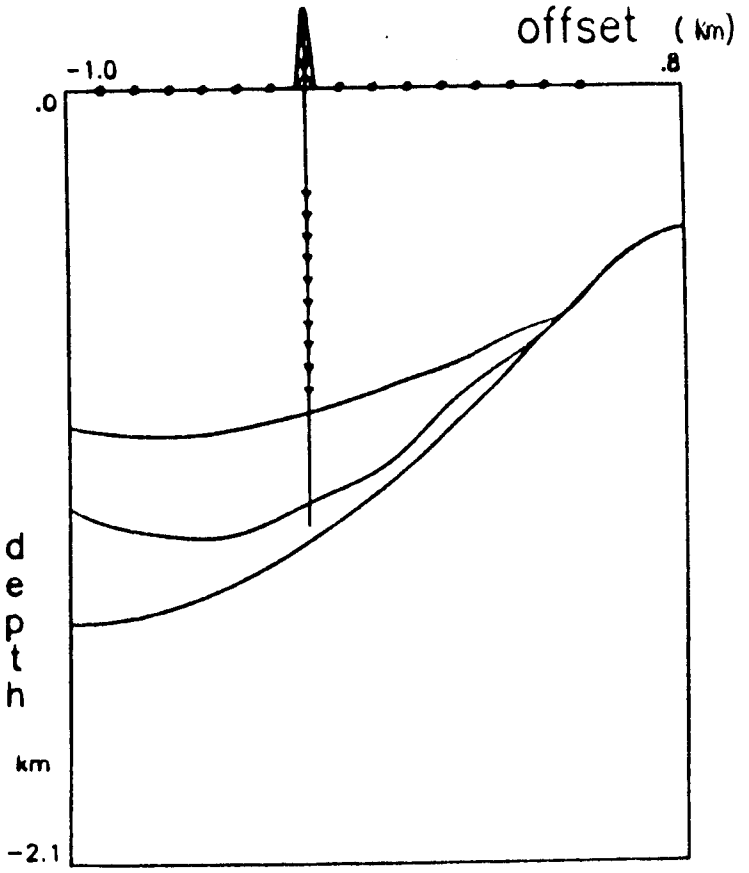

FIG. 13.a. Result of the first iteration of inversion. We can notice that layer three has become thinner.

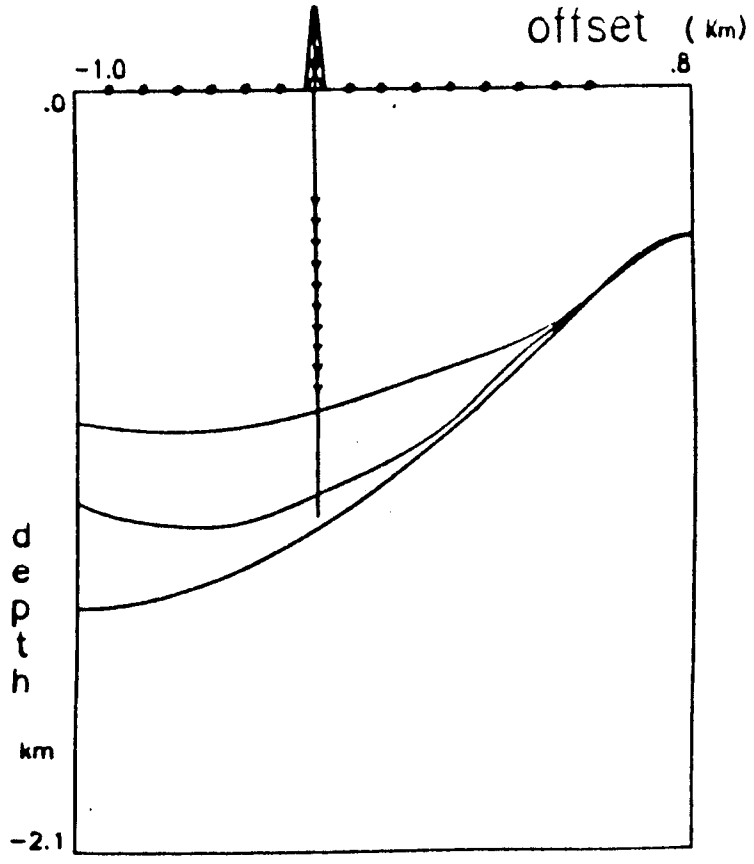

FIG. 13.b. The third iteration provides a good restitution of the correct position of the flank, where layers two and three are pinched out.

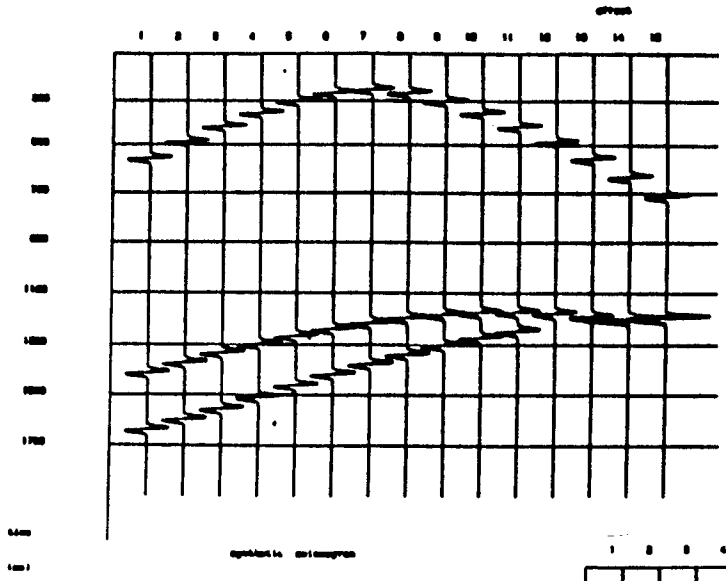

(a)

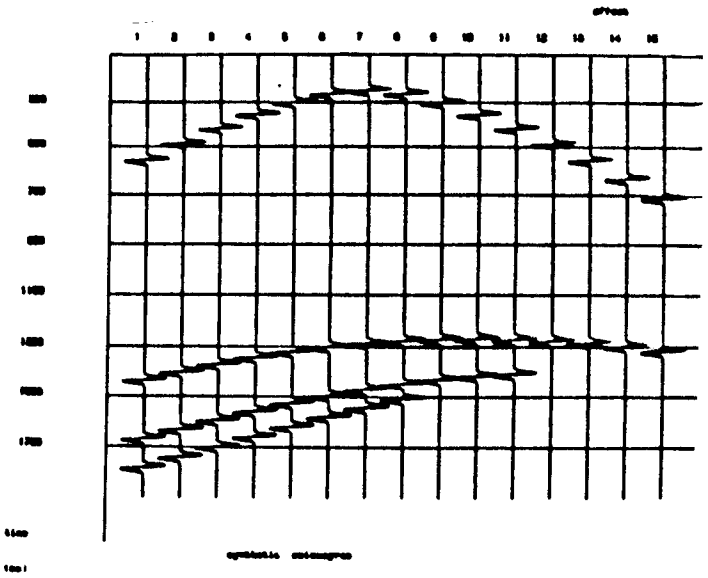

(b)

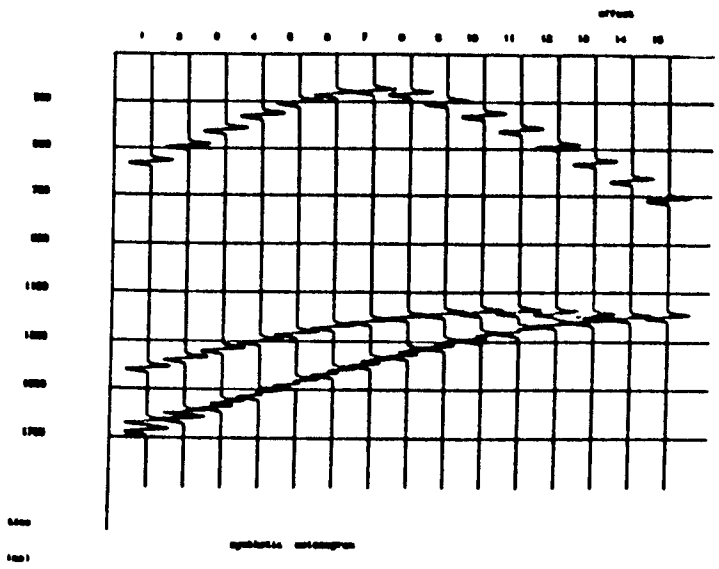

(c)

FIG. 14. Synthetic seismograms for example 2.
(a) correct model
(b) starting guess
(c) result of the inversion

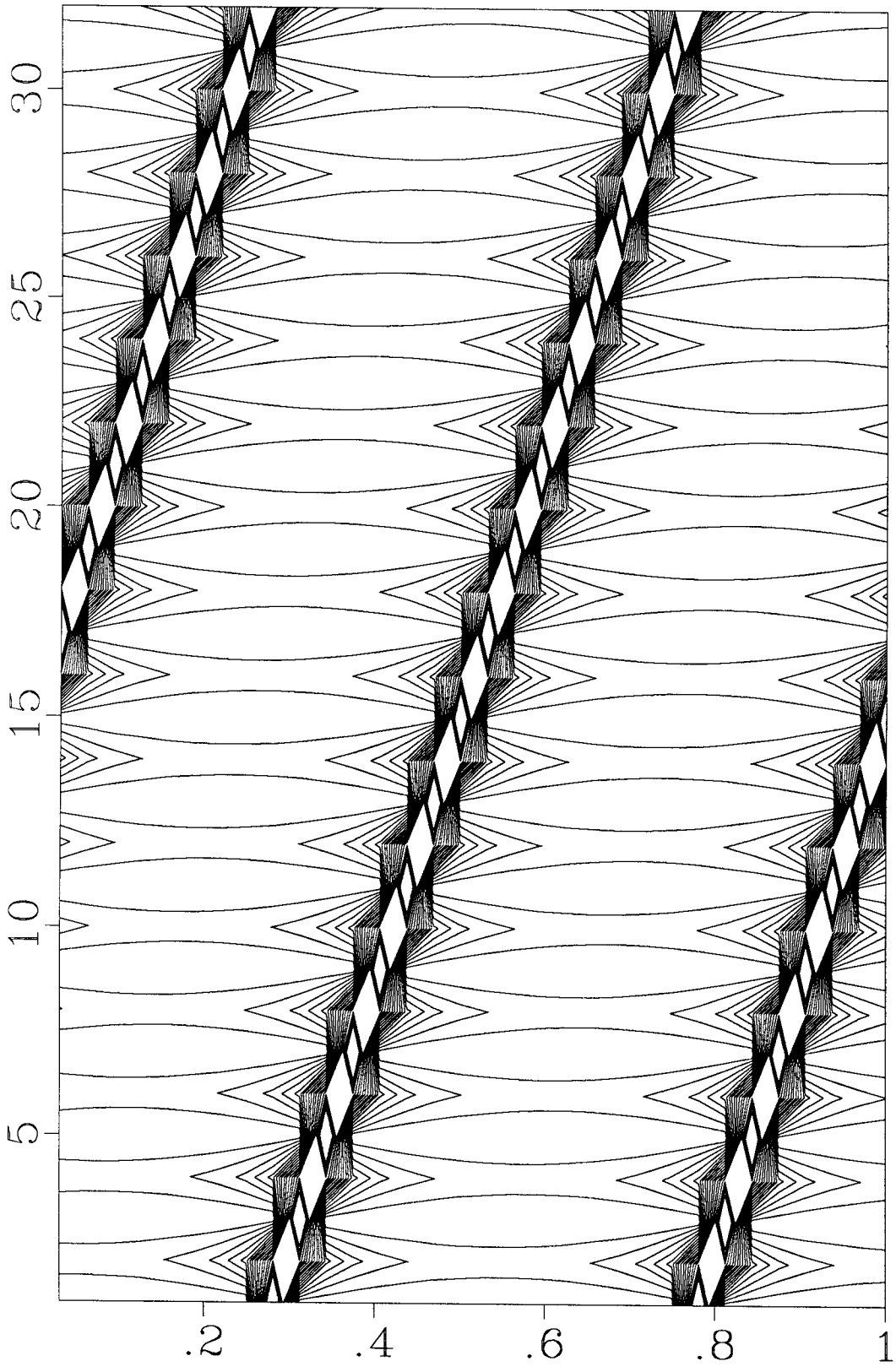
30
25
20
15
10
5
.2
.4
.6
.8
1